Preliminar Draft Version

Meta-modeling of Lattice Mechanical Responses via Design of Experiments

Diego Montoya-Zapata*†, Diego A. Acosta‡, Camilo Cortés†§, Juan Pareja-Corcho*, Aitor Moreno†§, Jorge Posada†§ and Oscar Ruiz-Salguero*
*Laboratory of CAD CAM CAE
Universidad EAFIT
Medellín, Colombia
†Vicomtech Foundation
San Sebastian, Spain
Email: ccortes@vicomtech.org
‡Grupo de Diseño y Desarrollo de Procesos (DDP)
Universidad EAFIT
Medellín, Colombia
§Basque Research and Technology Alliance (BRTA)
Mendaro, Spain

***Abstract*—In the context of lattice manufacturing, the problem of mechanical and structural characterization of large lattice domains is relevant. Lattice materials are used in engineering (e.g. in energy absorption and heat conduction) and biomedical (e.g. bone implants and artificial tissues) applications. However, the numerical simulation of large lattice domains is limited by its complicated geometry, which hinders the meshing stage and produces intractable finite element meshes. The existing efforts to simulate large lattice domains are based on the generation of simplified homogeneous domains equipped with material properties that approximate the behavior of the lattice domain equipped with the bulk material. Using this approach, one can estimate the displacements field over the lattice domain using a lighter mesh and a cheaper simulation. However, since stresses are influenced by geometrical conditions, the stresses of the simplified domain do not match the stresses of the lattice domain. As a response to this limitation, this article proposes a methodology based on the systematic use of design of experiments to devise meta-models to estimate the mechanical response of lattice domains. The devised meta-models can be integrated with material homogenization to allow the mechanical characterization of large lattice domains. In this paper, we apply the proposed methodology to develop meta-models for the estimation of the von Mises stress in Schwarz Primitive lattice domains. Results show that the proposed methodology is able to generate efficient and accurate meta-models whose inputs are based on the displacements on the boundary of the Schwarz cell. Therefore, numerical simulations with the homogeneous simplified domain can be used to feed the meta-models. Additional work is still required to integrate the developed meta-models with material homogenization to test large Schwarz Primitive lattice domains under working loads.**

***Index Terms*—response surface methodology, fractional factorial design, Plackett-Burman design, lattice structure, Schwarz Primitive**

GLOSSARY

AM:	Additive manufacturing.
CCF:	Central composite face-centered design.
CCI:	Central composite inscribed design.
DOE:	Design of experiments.
FEA:	Finite element analysis.
SIMP:	Solid isotropic material with penalization, which is a topology optimization algorithm.
SSE:	Sum of squared errors (SSE > 0).
R^2:	Coefficient of determination of the linear regression $\left(0 \leq R^2 \leq 1\right)$.
Ω, Ω^Q:	Subsets of $\mathbb{R}^3$ that represents the lattice domain and the equivalent homogeneous domain, respectively $\left(\Omega, \Omega^Q \subset \mathbb{R}^3\right)$.
E, E^Q:	Young's moduli of the bulk and equivalent material, respectively (Pa).
ν, ν^Q:	Poisson's ratio of the bulk and equivalent material, respectively.
σ_{VM}:	Von Mises stress (Pa).
L:	Length of the Schwarz Primitive cell $(L > 0)$.
ρ:	Relative density or volume fraction of a Schwarz Primitive cell $(0 \leq \rho \leq 1)$.
t:	Iso-value used to generate the Schwarz Primitive cell $(t \in [-3, 3])$.

I. INTRODUCTION

Recently, the interest on the development of functionally optimized and light materials has increased. This progress has been accompanied by the evolution of manufacturing technologies (e.g. 3D printing) that have made feasible the production of complex designs that used to be impossible to manufacture using subtractive techniques. In this context, the

numerical analysis of the new shapes and designs is key, since it reduces the time and money spent in test trials and physical experimentation.

Lattice structures are a kind of materials that point towards material and functional optimization: (i) the distribution of void/filled zones can be manipulated, which allows the optimization of mechanical properties, and (ii) can retain good mechanical properties while reducing material usage. However, Finite Element Analysis (FEA) of lattice structures is limited by their geometrical complexity, which produces intractable FEA meshes and impedes FEA simulation of large domains.

This manuscript implements an algorithm to estimate the stress/strain of lattice domains by systematically using Design of Experiments (DOE). We apply our algorithm to develop meta-models to approximate the von Mises stress in Schwarz Primitive lattice structures. The inputs of the devised meta-models are displacement-based features that can be obtained using material homogenization. The integration of the meta-models and material homogenization is not addressed in this work.

The remainder of this article is structured as follows: Section II provides a review of the related literature. Section III describes our algorithm to develop efficient meta-models for stress estimation in lattice domains. Section IV presents and discusses the results of applying the methodology for the estimation of the von Mises stress in Schwarz Primitive lattices. Section V concludes the manuscript and suggests future extensions of this work.

II. Literature Review

A. Material Homogenization in Lattice Structures

Lattice structures are families of materials formed by repetitive cells that are uniformly distributed throughout the design space. The main advantage of lattice structures is not only that they are lightweight, but also preserve good mechanical properties. Lattice structures are common in applications for energy absorption, heat transfer, vibration and acoustic damping [1]–[3].

The advent of additive manufacturing (or 3D printing) makes feasible the manufacturing of complex and customized lattice structures that resemble specific mechanical properties. Particularly, 3D printed lattice structures serve as customized bone implants [4], [5] or in other engineering applications to map the results of structural optimization into manufacturable (via additive manufacturing techniques) designs [6]–[8].

Material homogenization is the process of obtaining a homogeneous domain with equivalent properties that approximates the mechanical behavior of a lattice structure. Material homogenization alleviates the high computational costs of FEA simulations with large lattice domains. The simulation over the homogeneous domain is useful for estimating the displacement field of the lattice domain [7], [9]. However, the stress/strain on the homogenized domain differ of the stress/strain of the lattice domain, due to stress and strains are geometry-dependent properties.

B. Design of Experiments in FEA Modeling of Lattice Structures

In our literature survey we found that most finite element studies on lattice structures comprise domains of no more than a few hundred unit-cells [10]–[15]. Most analyses use beam elements to build the FEA model of lattice domains [10]–[13] with exception of a few studies that use tetrahedral [14] or shell elements [15]. We found very few studies with large domain size: Reference [16] presents a methodology to perform topology optimization on lattice domains with up to several million unit-cells (hollowed-square unit-cells).

Regarding the combined use of FEA simulations and DOE, we found that current work can be divided in two groups: (i) material properties evaluation, including metallic [17], resins [18] and composite materials [19], and (ii) shape optimization on mechanical parts, including medical devices [20], [21] and automobile parts [22]. To the best of our knowledge, the literature does not address the systematic application of DOE and material homogenization for stress estimation in the field of lattice materials.

C. Conclusions of the Literature Review

The literature review has shown that lattice structures are used in biomedical and engineering applications. Likewise, additive manufacturing has widen the application range of lattice structures, allowing the manufacturing of personalized prosthesis or implants. However, FEA of large lattice structures is still an open research question. The main limitation of the simulation of large lattice domains is its elevated computational cost. Its complicated geometry implies the use of small FEA elements which produces intractable FEA meshes.

To alleviate the computational burden of the simulation of lattice domains, material homogenization has been applied to produce simplified regular domains that approximate the original lattice domain. Despite the displacement field can be accurately estimated using this approach, the stress tensor cannot be directly obtained due to the geometric dissimilarities between the lattice and homogeneous domains.

In this paper, we aim to contribute to the problem of the estimation of the stresses in large lattice domains. We propose a methodology that uses DOE for the generation of simple mathematical expressions (meta-models) to characterize the stress/strain of lattice domains. The meta-models are designed so that their inputs can be later calculated by simulating the homogeneous domain.

Particularly, we develop meta-models to estimate the von Mises stress of Schwarz Primitive lattice structures using the strains of the boundary of the cell. The paper covers the whole pipeline of DOE, starting from a fractional factorial design for feature selection and the use of Response Surface and regression methods for obtaining the meta-models.

III. Methodology

A. Schwarz Primitive Lattice Structures

Schwarz Primitive cells are a kind of lattice structures that have been used in engineering and biomedical applications,

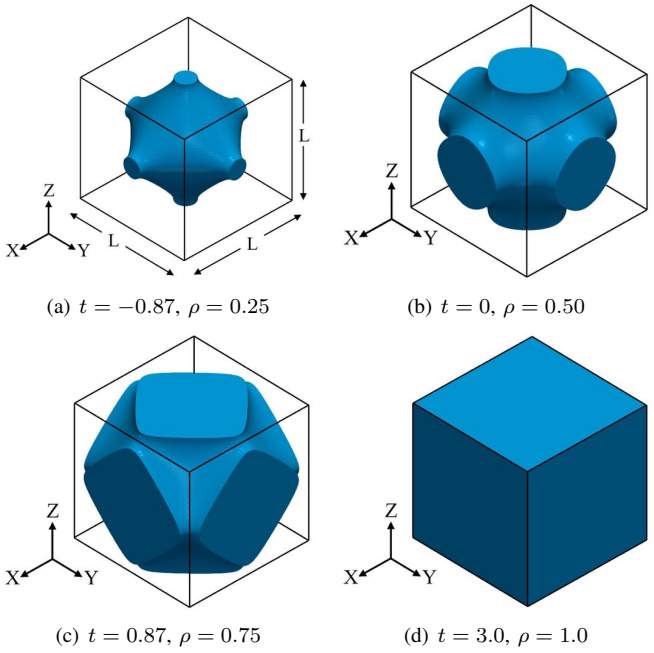

(a) $t = -0.87$, $\rho = 0.25$ (b) $t = 0$, $\rho = 0.50$

(c) $t = 0.87$, $\rho = 0.75$ (d) $t = 3.0$, $\rho = 1.0$

Fig. 1. Geometry and relative density of Schwarz Primitive cells for different isovalues.

and for the generation of manufacturable domains from the density maps produced by topology optimization [6], [8], [23]. The mechanical advantage of Schwarz Primitive cells is that they are stiffer than other basic lattice geometries [23].

Periodic domains of Schwarz Primitive cells are generated as isosurfaces of the scalar function $F(x, y, z)$ in Eq. 1:

$$F(x,y,z) = cos\left(\frac{2\pi}{L}x\right) + cos\left(\frac{2\pi}{L}y\right) + cos\left(\frac{2\pi}{L}z\right), \quad (1)$$

where L is the length of the cell [24]. Figure 1 shows the corresponding relative density ρ of different Schwarz Primitive cells generated with isovalues $t \in \{-0.87, 0.0, 0.87, 3.0\}$. The relative density ρ is the percentage of volume occupied by the cell with respect to the volume of the lattice L^3. Notice that larger isovalues produce cells with larger relative densities.

B. Generation of Meta-models using DOE

DOE is a well-established methodology based on statistical techniques that allows the analysis of complex processes and systems. The attractiveness of DOE lies on its ability to produce valuable conclusions while reducing the experimentation efforts [25], [26].

Particularly, we were interested in estimating the von Mises stress in Schwarz Primitive domains. The von Mises stress σ_{VM} is a material failure criterion defined as per Eq. 2:

$$\sigma_{VM} = \sqrt{\sigma_1^2 + \sigma_2^2 + \sigma_3^2 - (\sigma_1\sigma_2 + \sigma_1\sigma_3 + \sigma_2\sigma_3)}, \quad (2)$$

where $\sigma_1, \sigma_2, \sigma_3$ are the principal stresses. The criterion states that, for preventing failure, the von Mises stress must be below the tensile strength of the material.

In general, the process of meta-model development is divided into three steps: (1) identification of potential features (or factors) that affect the response variable, (2) selection of the main factors, that is, the factors that have most influence on the response variable, and (3) development of simple mathematical expressions that relates the main factors and the response variable (i.e. meta-models). Figure 2 shows the workflow for the development of meta-models for lattice structures. Below, we describe the general procedure to obtain meta-models using a DOE-based methodology and its application for the estimation of the von Mises stress in Schwarz Primitive lattices.

1) **Factors identification:** at this stage the analyst has to determine the features (or factors) $F_V = \{f_1, f_2, \cdots, f_n\}$ that affect the process and can be controlled. The process of factors identification depends on the expertise of the analyst to decide which are the factors that can characterize the response variable.
In our case, one of the goals was to develop meta-models that could be linked with material homogenization. Therefore, our factors had to be based on the displacement field, so that they could be retrieved from the FEA simulation over the homogeneous domain Ω^Q. Our set of factors were the strains ε_{ij} at the flat faces (extreme faces) of the boundary of a single Schwarz Primitive cell. For convenience, the flat faces were denoted as $\{X, -X, Y, -Y, Z, -Z\}$, where $\{-X, -Y, -Z\}$ are the flat faces at $x = 0, y = 0, z = 0$. Similarly, $\{X, Y, Z\}$ are the flat faces at $x = L, y = L, z = L$. We defined the strains at the flat faces as per Eq. 3:

$$\varepsilon_{ij} = \text{sgn}(i) \cdot \frac{U_{ij} - U_{-jj}}{L}, \quad i = \pm X, \pm Y, \pm Z, \quad j = x, y, z, \quad (3)$$

where U_{ij} represents the average displacement in j direction of the face i. For instance, U_{-Xy} is the displacement in y direction of the flat face at $x = 0$. Therefore, ε_{ij} is a measure of the strain of the face i in j direction. Observe that, based on Eq. 3, $\varepsilon_{-Xx} = \varepsilon_{-Yy} = \varepsilon_{-Zz} = 0$. This is necessary to avoid the introduction of strains due to pure translation. Our work is limited to the elastic zone of the material. Therefore, the range of the variables is $\varepsilon_{ij} \in [-0.007, 0.007]$.

2) **Factors selection:** the goal at this stage is to select the most relevant factors from the initial set of potential factors. In the context of DOE, full or fractional factorial designs are the preferred tools for factor selection. Since we were addressing a problem with a large number of factors (15), we used a special fractional factorial design: the Plackett-Burman design. In our case, the selected factors were then used to develop meta-models for the estimation of the von Mises stress for Schwarz Primitive lattice structures. The results of the Plackett-Burman design were analyzed in `R` [27].

3) **Meta-model development:** the goal at this stage is to develop efficient and simple mathematical expressions that expresses our response variable y as a function of the selected factors x_i. The outcome of this stage is a mathematical expression of this type (Eq. 4):

$$\hat{y} = \beta_0 + \sum_i \beta_i x_i + \sum_{i \leq j} \beta_{ij} x_i x_j, \tag{4}$$

where $\hat{y}$ is the predicted value of the response variable y and x_i are the input variables.
We used Response Surface methodologies (e.g. Central Composite designs or Box-Behnken design) to implement efficient designs that allowed the realization of the meta-models. We used regression analysis to estimate up-to second-order meta-models. The coefficients (β_i, β_{ij}) of the meta-models were estimated with the method of least squares in `R` [27]. We devised meta-models for Schwarz Primitive cells of relative densities $\rho = 0.25, 0.5, 0.75, 1.0$.

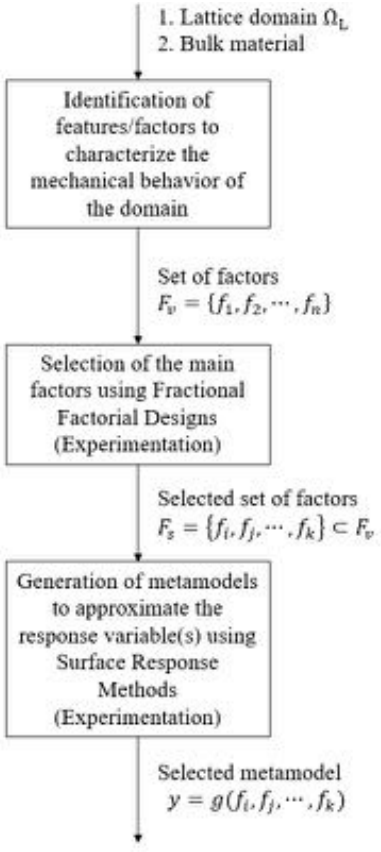

Fig. 2. Work-flow for the development of meta-models to approximate the mechanical response of lattice domains.

IV. Results

A. Material Homogenization in Lattice Structures

We implemented the numerical homogenization procedure presented in [28] to obtain the equivalent homogeneous properties for the Schwarz Primitive cells in Fig. 1. The length of each cell was $L = 2\pi$ cm. We chose the Titanium alloy *Ti-6Al-4V* as bulk material, with properties: Young's modulus $E = 114$ GPa and Poisson's ratio $\nu = 0.33$. The obtained equivalent properties for Schwarz Primitive cells at densities 0.25, 0.5, 0.75, and 1.0 are given in Table I.

TABLE I
Results of numerical homogenization of Schwarz Primitive cells: Young's modulus and Poisson's ratio.

Fig. number	Rel. density	Equivalent Young's modulus (E^Q)	Equivalent Poisson's ratio (ν^Q)
Fig. 1(a)	0.25	7.5 GPa	0.05
Fig. 1(b)	0.50	35.0 GPa	0.17
Fig. 1(c)	0.75	71.0 GPa	0.25
Fig. 1(d)	1.0	114.0 GPa	0.33

To evaluate the results of the homogenization procedure, we executed a compression test on a domain of eight Schwarz Primitive cells of density $\rho = 0.5$ (Fig. 3(a)). The compression load was 10 kN. We retrieved and compared the results of the x, y, and z displacements for (i) the lattice domain with the bulk material, and (ii) the homogeneous domain with the equivalent properties.

Results in Figs. 3(b)–3(g) show the agreement between the displacement fields of the lattice and homogeneous domains. It is important to remark that the FEA mesh of the lattice domain was composed by 132000 elements while the FEA mesh of the homogeneous domain had 8000 elements. This result shows the computational burden of simulating lattice domains, which encourages the use of more efficient approaches to estimate the mechanical response of large lattice domains, which could not be analyzed using conventional techniques.

B. Generation of the Meta-models

1) Selection of the Input Variables: We aimed to select the most relevant factors from the initial set of potential ones (Eq. 3). We used a Plackett-Burman design for this task. Initially, there were 15 factors defined on the flat faces of the Schwarz cell: (a) three normal strains

$$\{\varepsilon_{Xx}, \varepsilon_{Yy}, \varepsilon_{Zz}\}, \tag{5}$$

and (b) twelve shear strains

$$\begin{aligned}\{&\varepsilon_{Xy}, \varepsilon_{Xz}, \varepsilon_{-Xy}, \varepsilon_{-Xz}, \varepsilon_{Yx}, \varepsilon_{Yz},\\ &\varepsilon_{-Yx}, \varepsilon_{-Yz}, \varepsilon_{Zx}, \varepsilon_{Zy}, \varepsilon_{-Zx}, \varepsilon_{-Zy}\}.\end{aligned} \tag{6}$$

Given the number of factors (15 in total), we used a Plackett-Burman design with 20 runs. We executed the simulations with the cells of density $\rho = 0.25, 0.5, 0.75$ and side length $L = 10$ mm (Fig. 1). The cell of relative density $\rho = 1.0$ represented a special case due to its geometry, which did not allow the application of simultaneous normal and shear strains. Consequently, a different treatment was necessary to obtain the required meta-models (see Section IV-B2).

We evaluated the results of the Plackett-Burman design using (1) Bayes discrimination model determination [25],

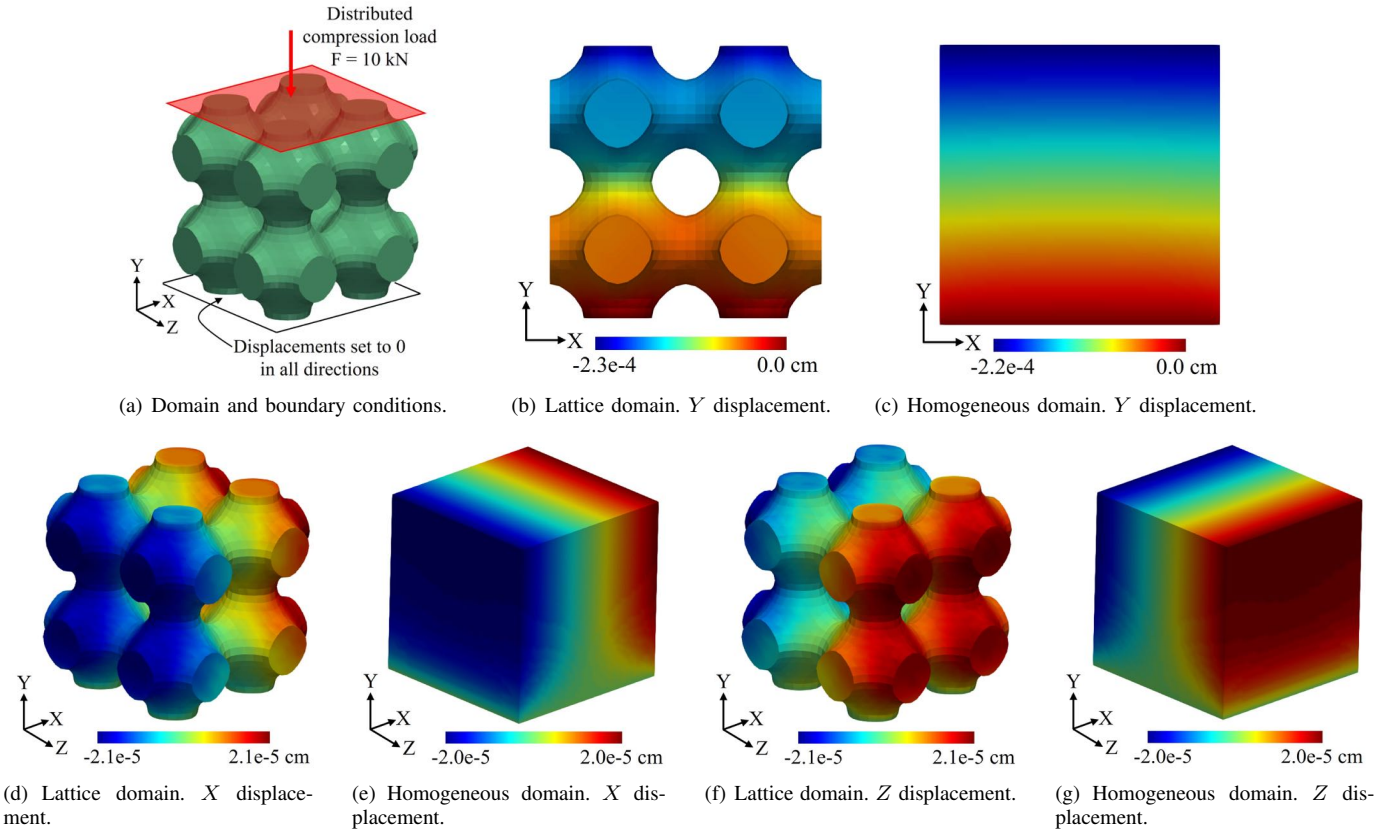

(a) Domain and boundary conditions. (b) Lattice domain. Y displacement. (c) Homogeneous domain. Y displacement.

(d) Lattice domain. X displacement. (e) Homogeneous domain. X displacement. (f) Lattice domain. Z displacement. (g) Homogeneous domain. Z displacement.

Fig. 3. Comparison of the displacement fields among the lattice and homogeneous domains for eight Schwarz Primitive cells.

and (2) Daniel's and Lenth's plots [26]. The analyses were implemented in `R`, with the package `BsMD` [29]. The results of these statistical analyses (provided in Fig. 4) show the similarity of the effects of all factors on the behavior of the von Mises stress in Schwarz Primitive domains. Based on this result, we conclude that all factors are relevant (no factor excels over the others) and they all have to be considered to build the meta-models. The development of the meta-models for the cells of density $\rho = 0.25, 0.5, 0.75$ is presented in Section IV-B3.

2) Meta-models for Schwarz Primitive Cell with Relative Density $\rho = 1.0$: Due to the cubic shape of the Schwarz Primitive cell of density $\rho = 1.0$, it was not possible to apply both normal and shear strains boundary conditions on the cell. Consequently, we devised the meta-models using only the normal strains (Eq. 5). For this task, we used the Response Surface methodology, specifically the Central Composite Face-centered (CCF) design. We fitted (1) first-order, (2) first-order plus iterations, and (3) second order models in terms of the normal strains ε_{Xx}, ε_{Yy}, and ε_{Zz} of the form

$$\hat{\sigma}_{VM} = \beta_0 + \sum_{i=1}^{3} \beta_i \varepsilon_{ii} + \sum_{i<=j}^{3} \beta_{ij} \varepsilon_{ii} \varepsilon_{jj}. \tag{7}$$

The value of the variables ε_{ij} was coded in the range $[-1, 1]$ to be in concordance with the procedures found in the literature [26]. Figure 5 shows the relation between the fitted and experimental values of the von Mises stress for 100 random simulations. For the simulated data, we calculated (1) the average of the relative error and (2) the sum of square errors (SSE) with the formula (Eq. 8)

$$SSE = \sum \left(\sigma_{VM} - \hat{\sigma}_{VM}\right)^2, \tag{8}$$

where σ_{VM} is the experimental von Mises stress and $\hat{\sigma}_{VM}$ is the predicted value. The corresponding values of the coefficients β_{ij}, R^2, SSE and the average relative error are given in Table II.

It is clear that the first-order and first-order plus interactions models do not fit well the data (the coefficient of determination R^2 is very low). For the second-order model, the coefficient of determination is very high $R^2 = 0.95$. However, Fig. 5(c) shows a clear trend in the error of the model. This trend becomes more obvious when plotting the residuals of the second-order model for the random simulations (Fig. 5(d)).

Due to the observed trend in the residuals of the second-order model, we developed meta-models for the square of the von Mises stress σ^2_{VM}. No further simulations were required for this task. It was only necessary to perform the regression analysis using $\hat{\sigma}^2_{VM}$ instead of $\hat{\sigma}_{VM}$ as the response variable in Eq. 7. The resultant meta-models and its performance are presented in Table III. Figure 6 depicts the predicted vs. the experimental values for σ^2_{VM}. The first-order and first-order plus iterations models do not fit the data and can be discarded.

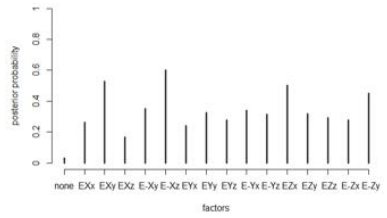

(a) Cell with $\rho = 0.25$. Bayesian analysis. Posterior probabilities.

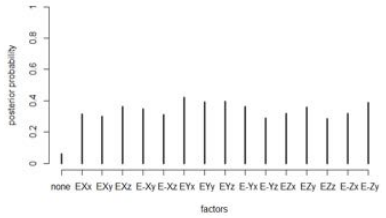

(b) Cell with $\rho = 0.5$. Bayesian analysis. Posterior probabilities.

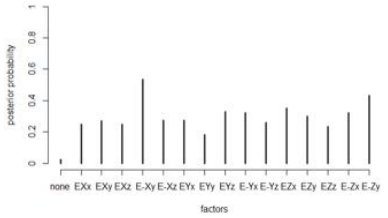

(c) Cell with $\rho = 0.75$. Bayesian analysis. Posterior probabilities.

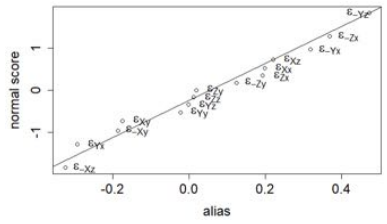

(d) Cell with $\rho = 0.25$. Daniel's plot.

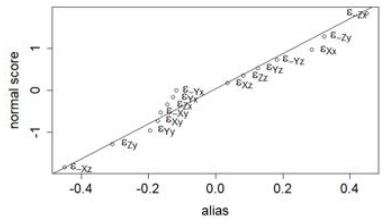

(e) Cell with $\rho = 0.5$. Daniel's plot.

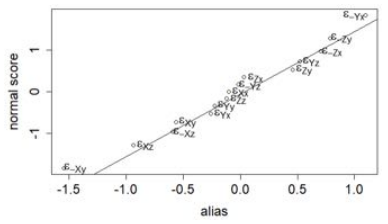

(f) Cell with $\rho = 0.75$. Daniel's plot.

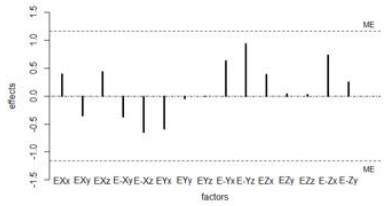

(g) Cell with $\rho = 0.25$. Lenth's plot.

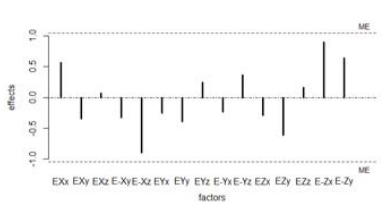

(h) Cell with $\rho = 0.5$. Lenth's plot.

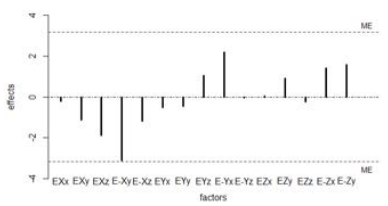

(i) Cell with $\rho = 0.75$. Lenth's plot.

Fig. 4. Results of the Plackett–Burman design for the Schwarz Primitive cells of relative density $\rho = 0.25$, $\rho = 0.5$ and $\rho = 0.75$. Bayesian analysis, Daniel's plot and Lenth's plot.

TABLE II
SCHWARZ PRIMITIVE CELL OF DENSITY $\rho = 1.0$. FITTED MODELS FOR THE VON MISES STRESS σ_{VM}.

Model	β_0	β_1	β_2	β_3	β_{12}	β_{13}	β_{23}	β_{11}	β_{22}	β_{33}	R^2	SSE	Avg. Rel. Error
First–order	0.8	0.0	0.0	0.0	N/A	N/A	N/A	N/A	N/A	N/A	0.00	12	126%
First–order + interactions	0.8	0.0	0.0	0.0	−0.3	−0.3	−0.3	N/A	N/A	N/A	0.71	7	87%
Second–order	0.8	0.0	0.0	0.0	−0.3	−0.3	−0.3	0.2	0.2	0.2	0.95	0.8	28%

On the other hand, it is noticeable the perfect fit of the second-order model. When expanding the mathematical formulation of the second-order model, we find that it has the following shape

$$\hat{\sigma}_{VM} = \sqrt{0.4\left(\varepsilon_{Xx}^2 + \varepsilon_{Yy}^2 + \varepsilon_{Zz}^2 - \left(\varepsilon_{Xx}\varepsilon_{Yy} + \varepsilon_{Xx}\varepsilon_{Zz} + \varepsilon_{Yy}\varepsilon_{Zz}\right)\right)}, \quad (9)$$

which is very similar to the formula for computing the von Mises stress in Eq. 9 using the principal stresses. This similarity is explained by the fact that the load directions coincide with the principal directions because only normal strains are being considered on a cubic geometry.

3) Meta-models for Schwarz Primitive Cell with Relative Density $\rho = 0.25, 0.5, 0.75$: So as for the cell of density $\rho = 1.0$, we generated meta-models using the Response Surface methodology. This methodology is well-suited only when the number of input factors is small (< 5). Therefore, we could not use the strains ϵ_{ij} at the flat faces of the boundary of the cell as direct inputs of the meta-models. We took advantage of the geometrical (cubic) symmetry of the Schwarz Primitive cells and defined two new variables X_1 and X_2 in terms of the strains on the flat faces ε_{ij}:

$$X_1 = |\varepsilon_{Xx}| + |\varepsilon_{Yy}| + |\varepsilon_{Zz}|, \quad (10)$$

$$\begin{aligned} X_2 = &|\varepsilon_{Xy}| + |\varepsilon_{Xz}| + |\varepsilon_{-Xy}| + |\varepsilon_{-Xz}| + \\ &|\varepsilon_{Yx}| + |\varepsilon_{Yz}| + |\varepsilon_{-Yx}| + |\varepsilon_{-Yz}| + \\ &|\varepsilon_{Zx}| + |\varepsilon_{Zy}| + |\varepsilon_{-Zx}| + |\varepsilon_{-Zy}|. \end{aligned} \quad (11)$$

We used the Central Composite Inscribed (CCI) design and the CCF designs [26] to generate several meta-models for the estimation of the von Mises stress of the cell. The absolute value of the variables ε_{ij} was coded in the range $[-1, 1]$ to be in concordance with the values in the literature [26]. The

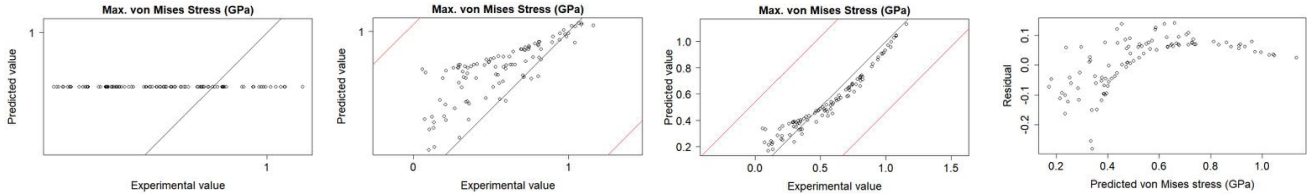

(a) CCF. First-order model. (b) CCF. First-order model plus interactions. (c) CCF. Second-order model. (d) CCF. Residuals of the second-order model.

Fig. 5. Evaluation of the fitted models for the Schwarz Primitive cell of density $\rho = 1.0$ for the von Mises stress. Fitted values vs. Experimental values.

TABLE III
SCHWARZ PRIMITIVE CELL OF DENSITY $\rho = 1.0$. FITTED MODELS FOR THE SQUARE OF THE VON MISES STRESS σ^2_{VM}.

Model	β_0	β_1	β_2	β_3	β_{12}	β_{13}	β_{23}	β_{11}	β_{22}	β_{33}	R^2	SSE	Avg. Rel. Error
First–order	0.8	0.0	0.0	0.0	N/A	N/A	N/A	N/A	N/A	N/A	0.00	19	160%
First–order + interactions	0.8	0.0	0.0	0.0	−0.4	−0.4	−0.4	N/A	N/A	N/A	0.57	14	128%
Second–order	0.0	0.0	0.0	0.0	−0.4	−0.4	−0.4	0.4	0.4	0.4	1.0	0	0%

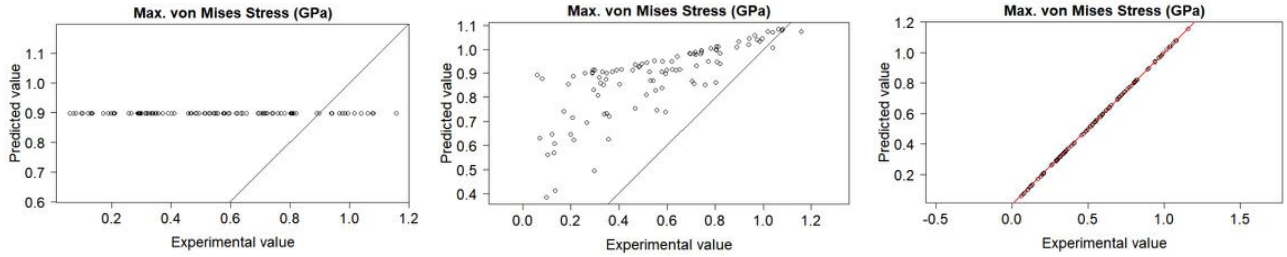

(a) CCF. First-order model. (b) CCF. First-order model plus interactions. (c) CCF. Second-order model.

Fig. 6. Evaluation of the fitted models for the Schwarz Primitive cell of density $\rho = 1.0$ for the square of the von Mises stress. Fitted values vs. Experimental values.

resultant meta-models for the cells of relative density $\rho = 0.25, 0.5, 0.75$ are listed in Tables IV–VI.

We evaluated the models using simulated data. We run 100 random simulations varying the values of the strain at the flat faces of the cell (ε_{ij}). Figures 7–9 show the graph of the predicted value of the von Mises stress $(\hat{\sigma}_{VM})$ vs. the experimental value (σ_{VM}). The red lines correspond to the interval of 99% of confidence using the standard deviation of each model.

Tables IV–VI report the SSE, the average of the relative error and the coefficient of determination R^2 for each model. In general, the R^2 of all models indicate a good fitting for the data used for adjusting the model. However, the data shown in Figs. 7–9 and the reported values of the SSE and the average relative error reveal that in both cases (CCI and CCF), the first-order and the first-order plus interactions models excel the second-order models.

V. CONCLUSIONS

This article presents a methodology to generate efficient meta-models to approximate the mechanical response of lattice materials using design of experiments. Particularly, the paper develops meta-models for the estimation of the maximum von Mises stress of Schwarz Primitive cells with relative densities $\rho = 0.25, 0.5, 0.75, 1.0$. The meta-models are obtained after conducting Plackett-Burman designs and Response Surface methodology. We obtained meta-models that fit adequately the data used for their generation. In the future, with the help of material homogenization, these meta-models could be used for estimating the von Mises stress of large Schwarz Primitive lattice domains composed cells under different loads (tension, compression, shear).

Our case study considers as features only the average strains in the flat faces of the boundary of each Schwarz Primitive cell. However, other features (e.g. the strain of the center of mass) can be evaluated. The selection of the best features to approximate the von Mises stress of Schwarz Primitive cells needs to be further investigated.

REFERENCES

[1] W. Hou, X. Yang, W. Zhang, and Y. Xia, "Design of energy-dissipating structure with functionally graded auxetic cellular material," *International Journal of Crashworthiness*, vol. 23, no. 4, pp. 366–376, 2018. [Online]. Available: https://doi.org/10.1080/13588265.2017.1328764

[2] K. J. Maloney, K. D. Fink, T. A. Schaedler, J. A. Kolodziejska, A. J. Jacobsen, and C. S. Roper, "Multifunctional heat exchangers derived from three-dimensional micro-lattice structures," *International Journal of Heat and Mass Transfer*, vol. 55, no. 9, pp. 2486 – 2493, 2012. [Online]. Available: https://doi.org/10.1016/j.ijheatmasstransfer.2012.01.011

TABLE IV
SCHWARZ PRIMITIVE CELL OF DENSITY $\rho = 0.25$. FITTED MODELS FOR THE VARIABLES X_1 AND X_2.

	Model	β_0	β_1	β_2	β_{12}	β_{11}	β_{22}	R^2	SSE	Avg. Rel. Error
CCF	First–order	9.6	0.9	0.5	N/A	N/A	N/A	0.94	627	18%
	First–order + interactions	9.6	0.9	0.5	−0.04	N/A	N/A	0.98	627	18%
	Second–order	8.7	0.9	0.5	−0.04	0.02	0.008	0.99	850	20%
CCI	First–order	9.1	0.5	0.3	N/A	N/A	N/A	0.98	710	19%
	First–order + interactions	9.1	0.5	0.3	−0.01	N/A	N/A	0.98	709	19%
	Second–order	8.5	0.5	0.3	−0.01	0.01	0.003	0.99	887	21%

TABLE V
SCHWARZ PRIMITIVE CELL OF DENSITY $\rho = 0.5$. FITTED MODELS FOR THE VARIABLES X_1 AND X_2.

	Model	β_0	β_1	β_2	β_{12}	β_{11}	β_{22}	R^2	SSE	Avg. Rel. Error
CCF	First–order	4.5	0.6	0.2	N/A	N/A	N/A	0.92	129	17%
	First–order + interactions	4.5	0.6	0.2	−0.02	N/A	N/A	0.97	128	17%
	Second–order	4.1	0.6	0.2	−0.02	0.006	0.004	0.99	215	24%
CCI	First–order	4.2	0.4	0.1	N/A	N/A	N/A	0.97	168	20%
	First–order + interactions	4.2	0.4	0.1	−0.004	N/A	N/A	0.97	167	20%
	Second–order	4.0	0.4	0.1	−0.004	0.002	0.002	0.98	214	23%

TABLE VI
SCHWARZ PRIMITIVE CELL OF DENSITY $\rho = 0.75$. FITTED MODELS FOR THE VARIABLES X_1 AND X_2.

	Model	β_0	β_1	β_2	β_{12}	β_{11}	β_{22}	R^2	SSE	Avg. Rel. Error
CCF	First–order	4.5	0.4	0.2	N/A	N/A	N/A	0.93	106	19%
	First–order + interactions	4.5	0.4	0.2	−0.02	N/A	N/A	0.98	105	19%
	Second–order	4.0	0.4	0.2	−0.02	0.03	0.003	0.99	127	20%
CCI	First–order	4.3	0.2	0.2	N/A	N/A	N/A	0.97	107	19%
	First–order + interactions	4.3	0.2	0.2	−0.008	N/A	N/A	0.98	107	19%
	Second–order	4.0	0.2	0.2	−0.008	0.01	0.002	0.99	125	20%

[3] S. Yin, L. Wu, J. Yang, L. Ma, and S. Nutt, "Damping and low-velocity impact behavior of filled composite pyramidal lattice structures," *Journal of Composite Materials*, vol. 48, no. 15, pp. 1789–1800, 2014. [Online]. Available: https://doi.org/10.1177/0021998313490582

[4] F. P. Melchels, K. Bertoldi, R. Gabbrielli, A. H. Velders, J. Feijen, and D. W. Grijpma, "Mathematically defined tissue engineering scaffold architectures prepared by stereolithography," *Biomaterials*, vol. 31, no. 27, pp. 6909 – 6916, 2010. [Online]. Available: https://doi.org/10.1016/j.biomaterials.2010.05.068

[5] A. Ataee, Y. Li, D. Fraser, G. Song, and C. Wen, "Anisotropic Ti-6Al-4V gyroid scaffolds manufactured by electron beam melting (EBM) for bone implant applications," *Materials & Design*, vol. 137, pp. 345 – 354, 2018. [Online]. Available: https://doi.org/10.1016/j.matdes.2017.10.040

[6] A. Panesar, M. Abdi, D. Hickman, and I. Ashcroft, "Strategies for functionally graded lattice structures derived using topology optimisation for Additive Manufacturing," *Additive Manufacturing*, vol. 19, pp. 81–94, 2018. [Online]. Available: https://doi.org/10.1016/j.addma.2017.11.008

[7] D. Li, W. Liao, N. Dai, G. Dong, Y. Tang, and Y. M. Xie, "Optimal design and modeling of gyroid-based functionally graded cellular structures for additive manufacturing," *Computer-Aided Design*, vol. 104, pp. 87 – 99, 2018. [Online]. Available: https://doi.org/10.1016/j.cad.2018.06.003

[8] D. Montoya-Zapata, A. Moreno, J. Pareja-Corcho, J. Posada, and O. Ruiz-Salguero, "Density-sensitive implicit functions using sub-voxel sampling in additive manufacturing," *Metals*, vol. 9, no. 12, 2019. [Online]. Available: https://www.mdpi.com/2075-4701/9/12/1293

[9] L. Cheng, P. Zhang, E. Biyikli, J. Bai, J. Robbins, and A. To, "Efficient design optimization of variable-density cellular structures for additive manufacturing: theory and experimental validation," *Rapid Prototyping Journal*, vol. 23, no. 4, pp. 660–677, 2017. [Online]. Available: https://doi.org/10.1108/RPJ-04-2016-0069

[10] P. Thiyagasundaram, J. Wang, B. V. Sankar, and N. K. Arakere, "Fracture toughness of foams with tetrakaidecahedral unit cells using finite element based micromechanics," *Engineering Fracture Mechanics*, vol. 78, no. 6, pp. 1277 – 1288, 2011. [Online]. Available: https://doi.org/10.1016/j.engfracmech.2011.01.003

[11] T. Zhong, K. He, H. Li, and L. Yang, "Mechanical properties of lightweight 316L stainless steel lattice structures fabricated by selective laser melting," *Materials & Design*, vol. 181, p. 108076, 2019. [Online]. Available: https://doi.org/10.1016/j.matdes.2019.108076

[12] H. Lei, C. Li, J. Meng, H. Zhou, Y. Liu, X. Zhang, P. Wang, and D. Fang, "Evaluation of compressive properties of SLM-fabricated multi-layer lattice structures by experimental test and μ-CT-based finite element analysis," *Materials & Design*, vol. 169, p. 107685, 2019. [Online]. Available: https://doi.org/10.1016/j.matdes.2019.107685

[13] J. A. Hawreliak, J. Lind, B. Maddox, M. Barham, M. Messner, N. Barton, B. Jensen, and M. Kumar, "Dynamic behavior of engineered lattice materials," *Scientific Reports*, vol. 6, no. 1, p. 28094, 2016. [Online]. Available: https://doi.org/10.1038/srep28094

[14] P. Terriault and V. Brailovski, "Modeling and simulation of large, conformal, porosity-graded and lightweight lattice structures made by additive manufacturing," *Finite Elements in Analysis and Design*, vol. 138, pp. 1 – 11, 2018. [Online]. Available: https://doi.org/10.1016/j.finel.2017.09.005

[15] C. Bonatti and D. Mohr, "Mechanical performance of additively-manufactured anisotropic and isotropic smooth shell-lattice materials: Simulations & experiments," *Journal of the Mechanics and Physics of Solids*, vol. 122, pp. 1 – 26, 2019. [Online]. Available: https://doi.org/10.1016/j.jmps.2018.08.022

[16] J. Wu, W. Wang, and X. Gao, "Design and optimization of conforming lattice structures," *IEEE Transactions on Visualization and Computer Graphics*, pp. 1–1, 2019. [Online]. Available: https://doi.org/10.1109/TVCG.2019.2938946

[17] T. Tryland, O. S. Hopperstad, and M. Langseth, "Design of experiments to identify material properties," *Materials & Design*, vol. 21, no. 5, pp. 477 – 492, 2000. [Online]. Available: https://doi.org/10.1016/S0261-3069(00)00035-2

[18] A. Kovalovs, A. Chate, S. Gaidukovs, and A. Medvids, "Finite element simulation of indentation experiment on branched epoxy novolac resin," *IOP Conference Series: Materials Science and Engineering*, vol. 500, p. 012006, 2019. [Online]. Available: https://doi.org/10.1088/1757-899x/500/1/012006

[19] L. Á. Oliveira, J. C. Santos, T. H. Panzera, R. T. Freire,

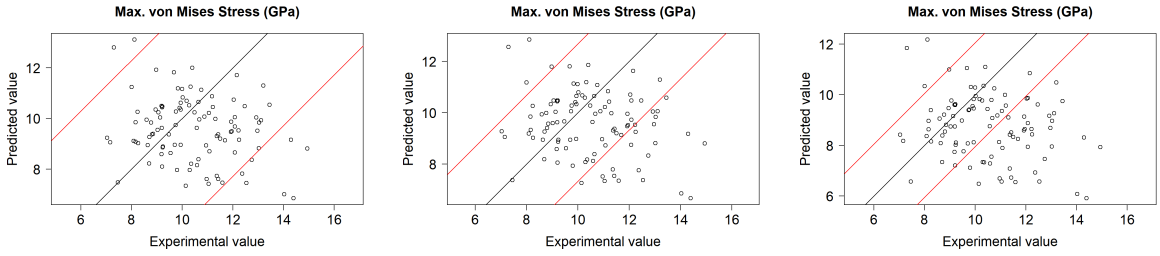

(a) CCF. First-order model. (b) CCF. First-order model plus interactions. (c) CCF. Second-order model.

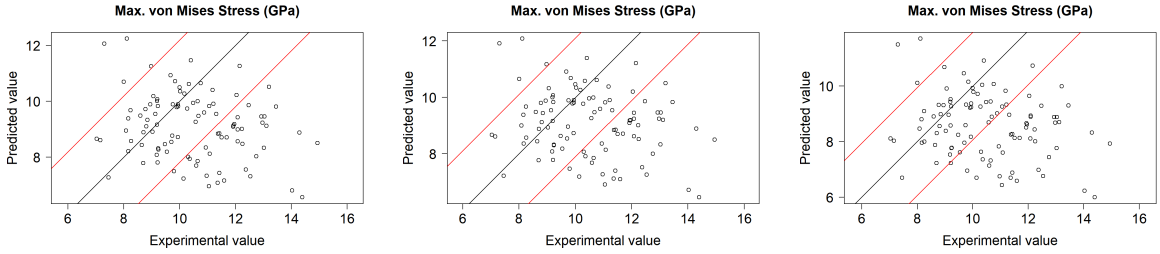

(d) CCI. First-order model. (e) CCI. First-order model plus interactions. (f) CCI. Second-order model.

Fig. 7. Evaluation of the fitted models for the Schwarz Primitive cell of density $\rho = 0.25$. Fitted values vs. Experimental values.

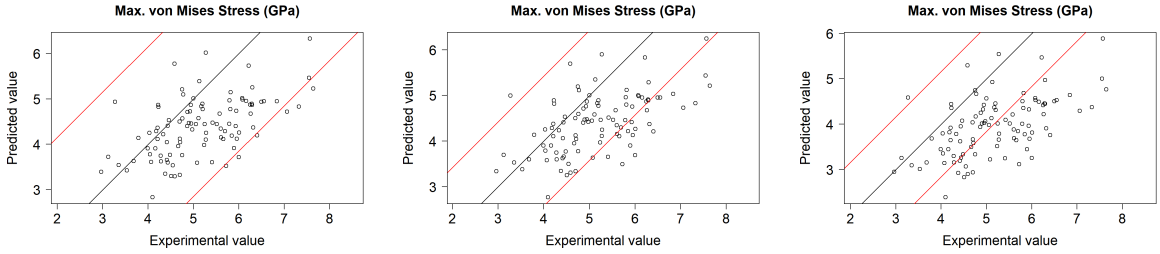

(a) CCF. First-order model. (b) CCF. First-order model plus interactions. (c) CCF. Second-order model.

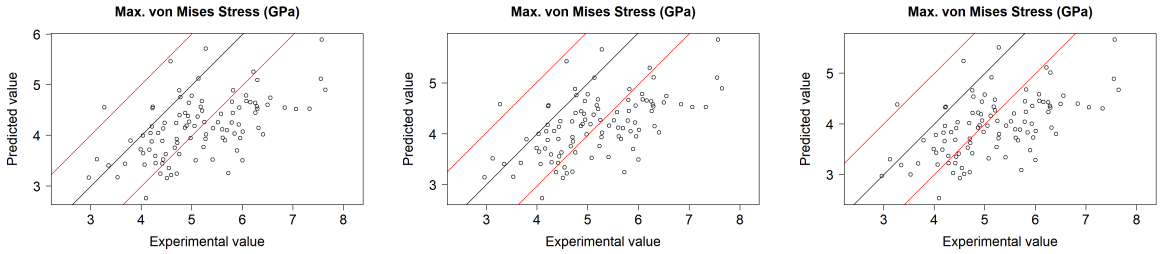

(d) CCI. First-order model. (e) CCI. First-order model plus interactions. (f) CCI. Second-order model.

Fig. 8. Evaluation of the fitted models for the Schwarz Primitive cell of density $\rho = 0.5$. Fitted values vs. Experimental values.

L. M. Vieira, and F. Scarpa, "Evaluation of hybrid-short-coir-fibre-reinforced composites via full factorial design," *Composite Structures*, vol. 202, pp. 313 – 323, 2018. [Online]. Available: https://doi.org/10.1016/j.compstruct.2018.01.088

[20] S. Phanphet, S. Dechjarern, and S. Jomjanyong, "Above-knee prosthesis design based on fatigue life using finite element method and design of experiment," *Medical Engineering & Physics*, vol. 43, pp. 86 – 91, 2017.

[21] W. C. Lee and M. Zhang, "Design of monolimb using finite element modelling and statistics-based Taguchi method," *Clinical Biomechanics*, vol. 20, no. 7, pp. 759–766, 2005. [Online]. Available: https://doi.org/10.1016/j.clinbiomech.2005.03.015

[22] C. Schäfer and E. Finke, "Shape optimisation by design of experiments and finite element methodsan application of steel wheels," *Structural and Multidisciplinary Optimization*, vol. 36, no. 5, pp. 477–491, 2008. [Online]. Available: https://doi.org/10.1007/s00158-007-0183-6

[23] I. Maskery, L. Sturm, A. Aremu, A. Panesar, C. Williams, C. Tuck, R. Wildman, I. Ashcroft, and R. Hague, "Insights into the mechanical properties of several triply periodic minimal surface lattice structures made by polymer additive manufacturing," *Polymer*, vol. 152, pp. 62 – 71, 2018, SI: Advanced Polymers for 3D Printing/Additive Manufacturing. [Online]. Available: https://doi.org/10.1016/j.polymer.2017.11.049

[24] M. Wohlgemuth, N. Yufa, J. Hoffman, and E. L. Thomas, "Triply periodic bicontinuous cubic microdomain morphologies by symmetries," *Macromolecules*, vol. 34, no. 17, pp. 6083–6089, 2001. [Online]. Available: https://doi.org/10.1021/ma0019499

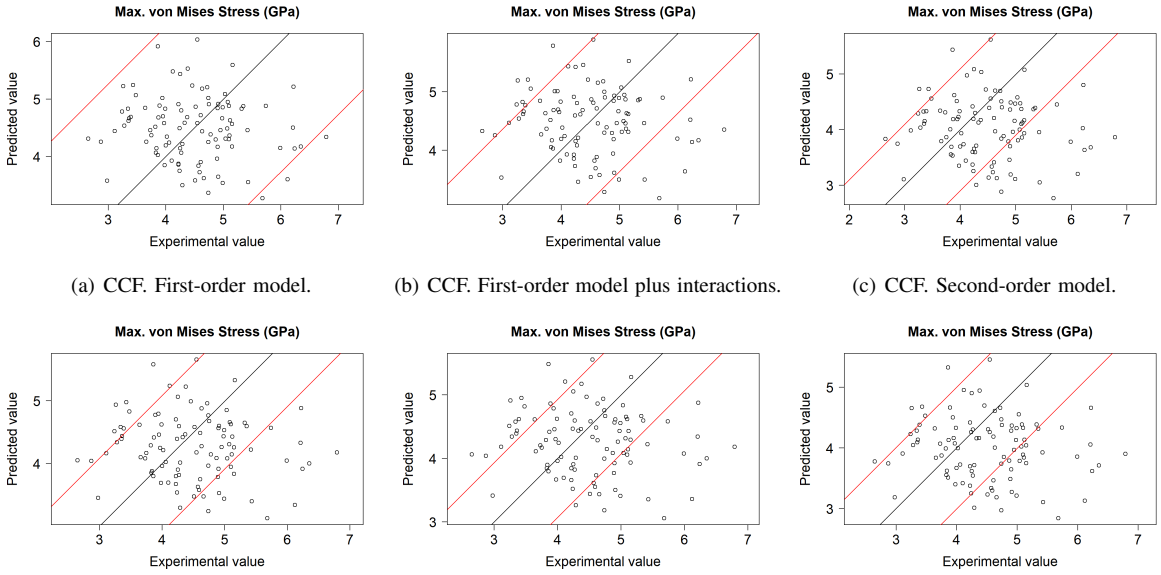

(a) CCF. First-order model. (b) CCF. First-order model plus interactions. (c) CCF. Second-order model.

(d) CCI. First-order model. (e) CCI. First-order model plus interactions. (f) CCI. Second-order model.

Fig. 9. Evaluation of the fitted models for the Schwarz Primitive cell of density $\rho = 0.75$. Fitted values vs. Experimental values.

[25] G. E. P. Box, J. S. Hunter, and W. G. Hunter, *Statistics for experimenters: design, discovery, and innovation*, 2nd ed., ser. Wiley Series in Probability and Statistics. Wiley, 2005.

[26] NIST/SEMATECH, "e-Handbook of Statistical Methods," http://www.itl.nist.gov/div898/handbook/. Accessed: 2019–12–04. [Online]. Available: http://www.itl.nist.gov/div898/handbook/

[27] R Core Team, *R: A Language and Environment for Statistical Computing*, R Foundation for Statistical Computing, Vienna, Austria, 2019. [Online]. Available: https://www.R-project.org/

[28] G. P. Steven, "Homogenization of multicomponent composite orthotropic materials using fea," *Communications in Numerical Methods in Engineering*, vol. 13, no. 7, pp. 517–531, 1997. [Online]. Available: https://doi.org/10.1002/(SICI)1099-0887(199707)13:7⟨517::AID-CNM74⟩3.0.CO;2-L

[29] E. Barrios based on Daniel Meyer's code., *BsMD: Bayes Screening and Model Discrimination*, 2018, R package version 2013.0718-1. [Online]. Available: https://CRAN.R-project.org/package=BsMD